



# Modelling groundwater recharge, actual evaporation and transpiration in semi-arid sites of the Lake Chad Basin: The role of soil and vegetation on groundwater recharge

Christoph Neukum<sup>1</sup>, Angela Gabriela Morales Santos<sup>2</sup>, Melanie Ronelngar<sup>3</sup>, Aminu Bala<sup>4</sup>, Sara Ines Vassolo<sup>1</sup>

<sup>1</sup> Federal Institute for Geosciences and Natural Resources, Department of Groundwater and Soil, Stilleweg 2, 30655 Hannover, Germany

<sup>2</sup> University of Natural Resources and Life Sciences, Vienna, Department of Water, Atmosphere and Environment, Institute for Soil Physics and Rural Water Management, Muthgasse 18, 1190 Vienna, Austria

<sup>3</sup> Federal Institute for Geosciences and Natural Resources at Lake Chad Basin Commission, Rond Point des Armes, Ndjamen, Chad

<sup>4</sup> Lake Chad Basin Commission, Rond Point des Armes, Ndjamen, Chad

Correspondence to: Christoph Neukum (christoph.neukum@bgr.de)

## Abstract.

The Lake Chad Basin, located in the center of North Africa, is characterized by strong climate seasonality with a pronounced short annual precipitation period and high potential evapotranspiration. Groundwater is an essential source for drinking water supply as well as for agriculture and groundwater related ecosystems. Thus, assessment of groundwater recharge is very important although difficult, because of the strong effects of evaporation and transpiration as well as limited available data.

A simple, generalized approach, which requires only a small number of field data, freely available remote sensing data as well as well-established concepts and models, is tested for assessing groundwater recharge in the southern part of the basin. This work uses the FAO-dual  $K_c$  concept to estimate E and T coefficients at six locations that differ in soil texture, climate, and vegetation conditions. Measured values of soil water content and chloride concentrations along vertical soil profiles together with different scenarios for E and T partitioning and a Bayesian calibration approach are used to numerically simulate water flow and chloride transport. Average groundwater recharge rates and the associated model uncertainty at the six locations are assessed for the 2003-2016 time-period.

Model results show that interannual variability of groundwater recharge is generally greater than the uncertainty of the modelled groundwater recharge. Furthermore, the soil moisture dynamics at all locations are limited rather by water availability for evaporation in the uppermost part of the soil and by water uptake in the root zone than by the reference evapotranspiration.

## 1 Introduction

The Lake Chad Basin (LCB) is one of the largest endorheic basins of the world with an area of approximately 2.5 million km<sup>2</sup>. The basin covers parts of Algeria, Cameroon, Central African Republic, Chad, Libya, Niger, Nigeria, and Sudan. According to the Lake Chad Basin Commission (LCBC, 2012), 45 million inhabitants are settled in the basin. The study areas Salamat



33 and Waza Logone are located in the southern part of the LCB along the Chari-Logone, the major tributary river system to the  
34 Lake Chad (Figure 1), which accounts for around 80-90% of the Lake Chad inflow (Bouchez et al., 2016).  
35 Groundwater is an important source for drinking water supply as well as for agriculture and groundwater related ecosystems  
36 in the LCB. The Lake Chad, the rivers, and the floodplains of the major rivers are characterized by strong seasonality, due to  
37 a pronounced short annual precipitation period and high potential evapotranspiration. Groundwater recharge, evaporation,  
38 transpiration, and the entire hydrological budget depend strongly on seasonality. However, the impact of transpiration as a  
39 potentially significant process of the hydrological budget (Jasechko et al., 2013) has not yet been intensively explored in the  
40 area (Bouchez et al., 2016).  
41 Many studies were published concerning the hydrological behaviour and budget of the Lake Chad, due to its substantial and  
42 frequent open water surface changes and related consequences to the population and the environment (e.g. Bouchez et al.,  
43 2016; Lemoalle et al., 2012; Olivry et al., 1996; Vuillaume, 1981). Another important topic associated to Lake Chad is  
44 groundwater recharge by infiltration of lake water into the Quaternary aquifer, which was estimated by isotopes studies (Fontes  
45 et al., 1969; Fontes et al., 1970; Gaultier, 2004; Zairi, 2008), water and salt budgets (Bader et al., 2011; Carmouze, 1972;  
46 Roche, 1980) or hydrogeological models (Isihoro et al., 1996; Leblanc, 2002). Local scale studies focusing on the hydrological  
47 processes in the vadose zone are largely missing in the LCB. Recently Tewolde et al. (2019) published such a study using  
48 stable isotope and chloride concentrations in partly the same soil profiles used in this work.  
49 For vadose zone studies, partitioning evapotranspiration (ET) into its respective soil evaporation (E) and plant transpiration  
50 (T) components is crucial for process-based understanding of fluxes (Anderson et al., 2017). There are a number of  
51 measurement and modelling approaches that can be used to estimate E and T separately. Some of the measurements include  
52 micro-lysimeter, soil heat pulse probes, Bowen ratio, and Eddy covariance to determine E; and sap flow, chambers, and  
53 biomass-transpiration relationship to measure T (Kool et al., 2014). Evapotranspiration partitioning can also be estimated  
54 directly by using stable isotopes to assess the ratio between E and T (Wu et al. 2016). Stable isotopes were used in combination  
55 with Eddy covariance on semi-arid environments as well (Aouade et al., 2016).  
56 The Food and Agricultural Organization of the United Nations (FAO) published a model (Allen et al., 1998) that uses an  
57 empirically defined crop coefficient ( $K_c$ ) in combination with a reference ET ( $ET_0$ ) to calculate crop evapotranspiration ( $ET_c$ ).  
58 There are two approaches for this method: single coefficient and dual crop coefficient. The FAO-dual  $K_c$  model is a validated  
59 method for ET partitioning and the most commonly applied (Kool et al., 2014). It has been widely used with good results for  
60 numerous crops under different conditions: e.g. wheat and maize in semi-arid regions (Shahrokhnia and Sepaskhah, 2013),  
61 wheat in humid climate (Vieira et al., 2016), cherry trees in temperate continental monsoon climate (Tong et al., 2016), irrigated  
62 eucalyptus (Alves et al., 2013), and canola in terrestrial climate (Majnooni-Heris et al., 2012).  
63 Quantification of water fluxes in the vadose zone and linking atmospheric water and solute input at the upper boundary of the  
64 soil with water and solute fluxes at different soil depths is frequently implemented using different type of models. Numerical  
65 models need information on vadose zone properties for accurate parametrization to link fluxes with state variables such as  
66 unsaturated hydraulic conductivity and water retention curve. Estimation of effective soil hydraulic parameters, which are



valid at the modelling scale, might be laborious. Furthermore, parameter estimation might vary significantly depending on the measurement method (Mertens et al., 2005), when water and solute fluxes dynamics are considered. Hydraulic and transport parameters obtained from inverse modelling can be ambiguous, if multiple parameters are simultaneously considered and boundary conditions are not well known. Combining different state variables of water flow and solute transport in one objective function was found to be a strategy for appropriate parametrization (Groh et al., 2018; Sprenger et al., 2015) and for the transient simulation of water and solute fluxes. However, large amount of data are necessary to obtain accurate estimates of state variables, which are rarely available in remote areas of Africa, and measurement of related variables are associated with a huge effort in such environments. Pedotransfer functions (PTF) bridge available and needed data and are frequently used to quantify soil parameters (van Looy et al., 2017; Vereecken et al., 2016). PTF strive to provide a balance between data accuracy and availability (Vereecken et al., 2016). Since PTF usually do not consider soil structure, their results are better for homogeneous soils than for structured ones (Sprenger et al., 2015; Vereecken et al., 2010).

Recharge occurs even in the most arid regions, mainly due to concentration of surface flow and ponding with lateral and vertical infiltration (Lloyd, 1986). Direct recharge by precipitation is possible in semi-arid regions, but intermittently, owing to the fluctuations in the periodicity and volume of precipitation that is inherent to such regions (Lloyd, 2009). Scanlon et al. (2006) synthesized recharge estimates for semiarid and arid regions globally. They found that recharge is sensitive to land use and cover changes, hence management of such changes are necessary to control recharge. Moreover, they stated that average recharge rates in semi-arid and arid regions range from 0.2 to 35 mm yr<sup>-1</sup>, representing 0.1 to 5% of long-term average annual precipitation. Edmunds et al. (2002) estimated direct recharge rates from precipitation in the Mangu Grasslands in NE Nigeria (western LCB) at rates between 16 mm year<sup>-1</sup> and 30 mm yr<sup>-1</sup>. Using the same method, they appraised the regional direct recharge for north Nigeria at 43 mm year<sup>-1</sup>, which highlights the importance of infiltration from precipitation to the groundwater table at regional scale. Recently, Cuthbert et al. (2019) investigated the relationship between precipitation and recharge in sub-Saharan Africa using multidecadal hydrographs. They found that focused recharge predominates in arid areas and is mainly controlled by intense rainfall and flooding events. Intense precipitation, even during years of lower annual precipitation, results in some of the largest years of recharge in dry subtropical locations.

The Chloride Mass Balance (CMB) approach is a widely used technique for estimating groundwater recharge. Edmunds and Gaye (1994) used interstitial water chloride profiles from the unsaturated zone, in combination with measurements of chemical parameters from dug wells samples, to calculate groundwater recharge in the Sahel (mean annual rainfall 1970-1990 around 280 mm). A recharge rate of 13 mm year<sup>-1</sup> over the studied area was obtained. They conclude that it is an inexpensive technique, which can be applied in many arid and semi-arid areas. Tewolde et al. (2019) applied the CMB on soil profiles of the LCB, which are partly used in this study. They estimated generally lower annual recharge in Salamat (3 to 19 mm year<sup>-1</sup>) compared to Waza Logone (50 to 118 mm year<sup>-1</sup>). One major difficulty of CMB is the choice of a representative chloride concentration, or the concentration that prevails at large depths, when evapotranspiration effects extinguish, particularly for soils with a strong vertical chloride concentration variability.



In general, time series of relevant data for estimating groundwater recharge is scarce in the LCB. A simple, generalized approach, which requires only a small number of field data, freely available remote sensing data, and well-established concepts and models is tested for assessing groundwater recharge in the semi-arid part of the LCB. This work applies the FAO-dual  $K_c$  concept to estimate E and T coefficients at six locations, which differ in soil texture, climate, and vegetation conditions. Measured values of soil water content and chloride concentrations along vertical soil profiles, partly published by Tewolde et al. (2019), together with different scenarios for E and T partitioning and a Bayesian calibration approach are used to numerically simulate water flow and chloride transport as well as produce time series of recharge. Average potential groundwater recharges and the associated model uncertainty are assessed for the 2003-2016 time-period.

## 2 Data and methods

### 2.1 Study sites

The LCB is a Mesozoic basin and a major part of its geology comprises sedimentary formations from the Tertiary and Quaternary periods (LCBC, 1993). The Quaternary sediments form a continuous layer of fluvial, lacustrine and aeolian sands. These medium to fine-grained sands act as an unconfined transboundary aquifer, as do all aquifers in the LCB, and are isolated from underlying aquifers by a thick layer of Pliocene clay (Leblanc et al., 2007; Vassolo, 2009). The Tertiary formation (Continental Terminal) consists of sandstones and argillaceous sands and is a classic example of a confined aquifer system that becomes artesian in the surroundings of the Lake Chad (Ngatcha et al., 2008). The availability of water from precipitation as well as the deposition characteristics of the aquifer play an important role in the recharge of the upper unconfined sands (Vassolo, 2009).

The study sites (Figure 1, Table 1) are located in the Salamat and Waza Logone floodplains in the southern Sahel zone and correspond to those published by Tewolde et al. (2019) for these areas, except for site ST4. Site ST4 is located far from any floodplain, which is the focus of this research, and its soil composition and vegetation are very similar to those from site ST3. Thus, including the location would not provide any additional information.

Sites ST1 and ST2 in Salamat as well as WL1 and WL3 in Waza Logone are annually flooded over three months, site WL2 located at the edge of the Waza Logone wetland is flooded only one month whereas site ST3, although close to ST1 in Salamat, is never flooded. In the Salamat region, mainly sorghum is grown with trees such as *Acacia albida*, *A. scorpioides* and *A. sieberana* present along the margins of the floodplains (Bernacsek et al., 1992). In the Waza Logone area, vegetation depends on the duration of submersion, being the grass savannahs flooded for longer periods of time (Batello et al., 2004).

### 2.2 Climate data

Monthly precipitation and potential evapotranspiration data from 1970 to 2019 for the specific sites in Salamat and Waza Logone are extracted from the CRUTS 4 database (Harris et al., 2020). The potential evapotranspiration is calculated using the Penman-Monteith method and is considered herein as the reference evapotranspiration ( $ET_0$ ). Wind speed at 10 m above



ground for Salamat and Waza Logone were obtained from Didane et al. (2017). To adjust these values for 2 m above ground, a correction factor of 0.7479 was applied, based on a logarithmic wind speed profile (Allen et al., 1998). Average annual precipitation in Salamat and Waza Logone are 807 mm and 709 mm, respectively. The rainy season is typically from May to September with maximum precipitations in July and August. Average annual values of  $ET_0$  are 1718 mm in Salamat and 2011 mm in Waza Logone, exceeding annual precipitation by more than twice. However, in the second half of the rainy season the monthly water balance is positive. The average water balance for July until September between 2003 and 2016 is  $131 \pm 101 \text{ mm month}^{-1}$  and  $90 \pm 63 \text{ mm month}^{-1}$  for Salamat and Waza Logone, respectively (Figure 2). Chloride concentration in ponding water was measured in four samples in Salamat. It varies between  $2.5 \text{ mg l}^{-1}$  and  $25 \text{ mg l}^{-1}$ . Precipitation was sampled using a Hellmann rainwater collector in N'Djamena. This device has been design to reduce to a minimum evaporation by using a narrow soft polypolypropylene plastic tube of 4 mm inner diameter to connect the funnel on top of the device with the bottom of the 3 l collection bottle (Gröning et al., 2012). Once precipitation starts, water rises in the bottle and into the tube decoupling the atmosphere from the bottle headspace to prevent evaporation. To ensure that evaporation is as low as possible, sampling took place event wise. Chloride concentration in precipitation was measured in 42 out of 147 samples collected in N'Djamena between 2014 and 2020 for different precipitation events and stages of the rainy season. Not all rain samples could be analyzed for chloride concentration, due to limited sample amount in minor events at the beginning and end of the rainy season. Average chloride concentration in May is  $2.5 \pm 2.3 \text{ mg l}^{-1}$  (3 samples). Precipitation in June to September have relatively low chloride concentrations declining from  $0.6 \pm 0.3 \text{ mg l}^{-1}$  to  $0.26 \pm 0.12 \text{ mg l}^{-1}$  and  $0.38 \pm 0.14 \text{ mg l}^{-1}$  at the end of the season. Strong rain events in July and August have chloride concentrations between 0.2 and  $0.3 \text{ mg l}^{-1}$ . The annual wet chloride deposition sums to  $1.8 \pm 0.5 \text{ kg ha}^{-1}$ . The measured values are in the range of published data (Goni et al., 2001; Laouali et al., 2012; Gebru and Tesfahunegn, 2019). Dry deposition of chloride is estimated between 10 – 30% of wet deposition (Bouchez et al. 2019).

### 2.3 Soil and vegetation data

At each study site, vertical soil profiles were core-drilled using a hand auger. In Salamat, soil profiles were sampled in 2016 (Tewolde et al., 2019) and 2019. In Waza Logone soil samples were sampled in 2017 only (Tewolde et al., 2019), due to security reasons in 2019. Each of the soil profiles were sampled in 10 cm intervals and filled into headspace glass vials and plastic bags. Each soil fraction was tested for grain size distribution using sieving and sedimentation standard procedures (Tewolde, 2017). Classification follows the soil texture triangle by the US Department of Agriculture (Šimůnek et al., 2011). Chloride concentration was analyzed after aqueous extraction from oven dried ( $105^\circ\text{C}$  for 24 hours) soil samples following the standard guideline DIN EN 12457-1 (Tewolde, 2017). Gravimetric water content is the mass of water contained in a sample as a percentage of the dried soil mass. It was obtained by weighting the moist sample, oven drying it at  $105^\circ\text{C}$  for 24 to 48 hours, and weighting it again. Since bulk densities were



not measured in the field, volumetric water contents are obtained multiplying the gravimetric water contents for each soil type and location by typical bulk densities obtained from the Global Gridded Surfaces of Selected Soil Characteristics database (Global Soil Data Task Group, 2000).

The type of vegetation and the annual cycle of crops, length of the flooding period, and vegetation throughout the dry period were mapped during field work and documented by surveying resident population. In addition, MODIS vegetation indices data (Didan, 2015) were used to justify the documented annual cycle of phenology (Figure 3).

### 3 Modelling methodology

Our approach assumes that groundwater recharge is controlled by precipitation, evaporation, and transpiration (surface runoff can be neglected due to the flat topography). Soil moisture and chloride concentration along the soil profile at a certain time are indicators for evaporation and transpiration processes within the root zone of soils. Chloride concentration in soil depends on its input via precipitation and washing out of dry deposition as well as on the amount of evaporation and transpiration on the soil surface and in the root zone.

The first estimation of evapotranspiration was carried out using the FAO-dual crop coefficient approach that assesses E and T individually. The uncertainty of E and T partitioning on soil water and chloride concentration in the six soil profiles was assessed by considering scenarios of mean, maximum, and minimum E and T coefficient (see 3.1). Calculated time series of E and T for the site-specific vegetation were used to estimate soil water and chloride concentration profiles at the sampling time in each of the six locations using Hydrus-1D. A Bayesian approach was applied to consider uncertainties in chloride concentrations of precipitation and dry deposition, in partitioning E and T as well as in the parametrisation of the soil hydraulic model.

#### 3.1 Partitioning of evaporation and transpiration

Evapotranspiration (ET) is the combination of two main processes driven by atmospheric demand: evaporation from the soil (E) and transpiration through the stomata of plants (T) and is an important component of the water balance, especially in semi-arid areas. The FAO provides a model (Allen et al., 1998) for estimating crop evaporation ( $ET_c$ ) based on an empirically defined crop coefficient ( $K_c$ ) combined with a reference evapotranspiration ( $ET_0$ ). Two approaches are possible, single crop coefficient and dual crop coefficient. The latter was applied in this work.

The dual  $K_c$  method (Allen et al., 1998) is the sum of two coefficients, the basal crop coefficient ( $K_{cb}$ ) that describes plant transpiration and the soil water evaporation coefficient ( $K_e$ ) that depicts evaporation from the soil surface.  $K_{cb}$  is defined as the ratio of crop evapotranspiration over reference evapotranspiration ( $ET_c/ET_0$ ), when the soil surface is dry and transpiration occurs at a potential rate (i.e. unlimited water availability for transpiration).  $K_e$  is maximal when the topsoil is wet, but diminishes with drying out of topsoil to become zero, if no water remains near the soil surface for evaporation.

The parameters required for the estimation of monthly  $ET_c$  are the monthly reference evapotranspiration ( $ET_0$ ), the monthly basal crop coefficient ( $K_{cb}$ ) and the monthly soil water evaporation coefficient ( $K_e$ ):



$$ET_c = ET_0 * K_c = ET_0 * (K_{cb} + K_e), \quad (2)$$

Onsite information on vegetation and phenology, such as month of planting, full emergence of crop, and harvesting was used to define the monthly variation of vegetation at the study sites. These different vegetation periods were combined with crop specific Kcb for sorghum and grass provided in Allen et al. (1998) for sub-humid climate with relative humidity of 45% and average moderate wind speed of 2 m s<sup>-1</sup>. To comply with the local semi-arid climate conditions in Salamat and Waza Lagone, the coefficients Kcb for mid and end vegetation periods were adjusted as proposed by Allen et al. (1998). Monthly Kcb values for acacia were estimated based on Do and Rocheteau (2003) and Do et al. (2008). Site-specific monthly variation of ground cover and flooding periods with ranges of crop coefficient (Kcb), soil water evaporation coefficient (Ke), and root depth are provided in Table S1.

### 3.2 Modelling water flow and solute transport

#### 3.2.1 Model concept, setup, and initial conditions

The chloride profiles measured in soil at a certain time represent the input history for water and solute budget from past precipitation events and can be estimated by transient water flow and solute transport modelling. The model concept assumes that atmospheric chloride input is restricted to solute in precipitation and that the chloride concentration profile results from solute enrichment in the soil, due to evaporation and transpiration. A precise parametrization of the unsaturated flow and transport model as well as a robust quantification of groundwater recharge are not possible with the available data and hence cannot be the scope of this study. However, the model results estimate groundwater recharge magnitude and variability based on information regarding soil texture and vegetation as well as associated results uncertainty. This proposed approach is appropriate for locations with limited availability of long-term soil water measurements.

The free software package Hydrus-1D version 4.17.0140 was used to simulate transient water flow and solute transport in the six variably saturated soil profiles. Hydrus-1D numerically solves the Richards (1931) equation for variably saturated water flow, advection-dispersion equations for heat, and solute transport (Šimůnek et. al, 2009):

$$\frac{\partial \theta(h)}{\partial t} = \frac{\partial}{\partial z} \left[ K(h) \left( \frac{\partial h}{\partial z} + \cos \alpha \right) \right] - S(h) \quad (3)$$

with:

h	soil water pressure head [L]
θ	volumetric water content [L <sup>3</sup> L <sup>-3</sup> ]
t	time [T]
z	spatial coordinate [L] (positive upwards)
S	sink term [L <sup>3</sup> L <sup>-3</sup> L <sup>-1</sup> ]
α	angle between flow direction and vertical axis
K(h)	unsaturated hydraulic conductivity function [LT <sup>-1</sup> ]



The processes simulated in the six research sites were water flow, solute transport, and root water uptake. Because Hydrus-1D calculates with daily time step and data were only available at monthly scale, daily rates were calculated by dividing monthly data by month-specific days and assumed constant over the whole month. Model running ended at the soil sampling time (December 2016 and July 2019 for Salamat and June 2017 for Waza Logone). Progressive root growth was considered in all profiles except for ST2, in which the roots of the acacia trees were distributed along the whole profile and assumed invariant over the simulation period. Since initial conditions of soil moisture and resident chloride concentration are unknown, arbitrary values were adopted. To account for different residence times of water and chloride, due to different degrees of evapotranspiration and unknown initial conditions, each model was run over a period of time long enough to allow the exchange of at least one water column volume. Thus, total modelling periods are different depending on soil type at site: ST1, ST2 start in 1910, ST3 in 2010, WL1 and WL2 in 1990, and WL3 in 1970. All profiles were discretized into 101 nodes and different horizons according to the soils types interpreted from the individual grain size distributions.

### 3.2.2 Water flow

For calculation of water retention ( $\theta$ ) and unsaturated hydraulic conductivity functions ( $K(h)$ ), the Mualem-van Genuchten (MVG) model (van Genuchten, 1980) was applied:

$$\theta(h) = \begin{cases} \theta_r + \frac{\theta_s - \theta_r}{[1 + |\alpha h|^n]^m} & h < 0 \\ \theta_s & h \geq 0 \end{cases} \quad (4)$$

$$k(h) = k_s Se^{-1} [1 - (1 - Se^{l/m})^m] \quad (5)$$

where:

$$m = 1 - \frac{1}{n}; \quad n > 1$$

$$Se = \frac{\theta(h) - \theta_r}{\theta_s - \theta_r}$$

with

$\theta$  water content [-]

$h$  hydraulic head [L]

$\theta_r$  residual water content

$\theta_s$  saturated water content

$\alpha$  inverse of the air-entry value, empirical [ $L^{-1}$ ]

$n$  pore-size distribution index, empirical [-]

$l$  pore-connectivity parameter, empirical  $\approx 0.5$  [-]

$Se$  effective saturation [-]



The initial parametrization of these functions was realized using pedotransfer functions implemented in Rosetta (Schaap et al., 2001), which is a dynamically linked library coupled to Hydrus-1D. The input parameters for each profile were the percentages of sand, silt, clay, and bulk density at several depths. Whenever consecutive layers of a profile showed almost the same grain distribution (texture) and soil moisture, the layers were lumped in one and parameter averages were used in the model. The tortuosity parameter  $\tau$  of the MVG was set to 0.5 as proposed by Mualem (1976). The upper boundary condition was defined as variable atmospheric condition, whereas the lower one was set to zero-gradient with free drainage of water for all profiles, except WL3 where confined groundwater conditions prevailed below the confining clay layer encountered at 3.9 m depth. During drilling, groundwater was hit at 3.9 m depth, but rapidly rose to 2.6 m below surface. Consequently, a constant head condition was implemented at 2.6 m depth.

### 3.2.3 Root water uptake and root growth

The sink term ( $S$ ) in the Richards' equation, defined by Feddes et al. (1978) as the volume of water removed from a unit volume of soil per unit time due to plant water uptake, was considered in all soil profiles according to the prevailing vegetation (Table S1). The Feddes' default parameters for grass were used in ST3 and Waza Logone profiles. In ST1, where sorghum was planted, Feddes' parameters for corn were used because sorghum is not available in the list. According to Righes (1980) sorghum and corn roots extract water from approximately the same soil depths and have similar average root density distribution.

An average root depth of 1 m was adopted in ST1 for the initial and end seasons, and 2 m for development and mid seasons. In the case of acacia in ST2, the adopted parameters correspond to deciduous trees. The root depth of the acacia tree was considered as constant over the whole simulation period with maximum root distribution at 0.5 m and decreasing distribution down to 2 m (Beyer et al., 2016). In ST3, the vegetation was defined as grass, while in WL1, WL2 and WL3 as grass with a flooding period of 3 months in WL1 and WL3, but only one month in WL2. Rooting depth values used in these sites range from 0.1 m to 0.5 m, depending on the growth stage of grass. The median maximum rooting depth value of annual grass in water-limited ecosystems is 0.37 m with a 95% of confidence in an interval of 0.26 m-0.55 m (Schenk and Jackson, 2002).

### 3.2.4 Solute transport

The chloride concentration in soil water was simulated using an equilibrium advection-dispersion model implemented in Hydrus1-D. Hydrodynamic dispersion was implemented considering dispersivity values of 10% of the individual layer thickness in the soil model, a molecular diffusion coefficient of  $1.3 \times 10^{-9} \text{ m}^2 \text{ s}^{-1}$ , and a tortuosity factor as defined by Millington and Quirk (1961). Adopted dispersivity values are within reported ranges of 0.8 cm to 20 cm (Vanderborght and Vereecken, 2007; Stumpp et al, 2009, 2012).

A time-dependent concentration boundary condition was applied to the upper boundary and a zero-gradient boundary condition to the lower boundary. The transient liquid phase concentration of infiltrating water follows measured chloride concentration



in precipitation sampled in N'Djamena. Chloride concentration of ponding water correspond to four values measured in Salamat that range from 2.5 mg l<sup>-1</sup> to 25 mg l<sup>-1</sup> with an average of 9 mg l<sup>-1</sup>.

### 3.2.5 Crop evapotranspiration scenario definition

Since crop evapotranspiration was not measured, values were simulated using K<sub>cb</sub>, K<sub>e</sub>, and root depth instead. Because these parameters are given in ranges (Table S1), seven scenarios with different combination of K<sub>cb</sub>, K<sub>e</sub>, and root depth were developed to assess ranges of crop evaporation (Table 2). Scenario “Mean” corresponds to the average value of all parameters. Scenarios “Min” and “Max” combine the minimum and maximum values, respectively. Scenario “Mix-1” combines minimum K<sub>cb</sub> with average K<sub>e</sub> and root depth, scenario “Mix-2” minimum K<sub>e</sub> with average K<sub>cb</sub> and root depth whereas scenario “Mix-3” combines minimum root depth with average K<sub>e</sub> and K<sub>cb</sub>.

### 3.2.6 Bayesian model calibration

Based on the crop evapotranspiration scenarios, the models were calibrated and model uncertainty was estimated using a Bayesian calibration. Bayesian analysis is a combination of the data likelihood and the prior distribution using the Bayes theorem (ter Braak and Vrugt, 2008). The sum of likelihood functions for soil moisture and chloride concentration was implemented to calculate the log-likelihood of a simulation given the observations and standard deviations at each calibration step. The posteriori parameter distribution was estimated using the Differential Evolution Markov Chain Monte-Carlo (DE-MCz) algorithm with three sub-chains (ter Braak and Vrugt, 2008) implemented in the R package BayesianTools (Hartig et al., 2019). The number of iterations was defined individually according to a Gelman-Rubin reduction factor < 1.2. In the calibration, scaling factors ranging from 0.75 to 1.25 for the MVG parameters (saturated volumetric water content, alpha, and n) were adopted individually. However, ranges for MVG model parameter n were constraint to n > 1.01. Log-transformed saturated hydraulic conductivity for each layer was considered with ranges from -0.5 to 0.5. The scaling factor for transpiration was used as divisor for evaporation simultaneously to remain within the calculated rate of ET<sub>0</sub>. From all accepted model runs, 100 were randomly selected at each individual location to evaluate average model results and standard deviations.

## 4 Results

### 4.1 Grain size distribution

Soil textures were defined based on grain size distributions of the six profiles (Figure 4) according to the US Department of Agriculture soil texture triangle. Most of them are fine-grained soils (clay, sandy clay) and fine-grained soils with intercalation of thin sand and loam layers. Only soil profile ST3 is dominated by sand and sandy clay loam.



## 315 4.2 Model parametrization

316 The calibrated parametrization of the MVG model for each layer of the six sampling locations are plausible (Table 3). The  
 317 posterior distributions of the Bayesian calibration show the sensitive parameters of the model fit. For ST1, these are  $n$ , saturated  
 318 water content, chloride concentration, and the transpiration fraction in evapotranspiration, but the saturated hydraulic  
 319 conductivity is less sensitive (Fig. S1). For ST2, the sensitivities of the model parameters are similar with the saturated  
 320 hydraulic conductivity of the upper layer being sensitive and the influence of chloride concentration being less significant (Fig.  
 321 S2) compared to the other locations. The model fits of the data from site ST3 are generally insensitive. Only the model  
 322 parameters  $\alpha$ ,  $n$ , and saturated hydraulic conductivity of the upper layer as well as chloride concentration in precipitation  
 323 show tighter posteriori distributions (Fig. S3). For site WL1, the model parameters  $n$  of layers 1, 2, and 3 and as well as the  
 324 saturated water content of layers 3 and 5, and subordinately of layer 4, are sensitive. The parameters  $\alpha$  for layers 1 to 5,  
 325 the chloride concentration, and the fraction of transpiration are hardly sensitive in the range of the prior distribution (Fig. S4).  
 326 For WL2, the model parameters  $n$  of all layers, the saturated hydraulic conductivity of layer 3, and the saturated water content  
 327 of layers 2 and 3 are sensitive (Fig. S5). For WL3, the saturated water contents of layer 2, the saturated hydraulic conductivity  
 328 of layers 1 and 2, and the fraction of transpiration in evapotranspiration are sensitive (Fig. S6).

## 329 4.3 Soil water content, chloride concentration and groundwater recharge

330 Measured and simulated water content and chloride concentration profiles for individual scenarios are shown in Fig. 5. The  
 331 average root mean squared error (RMSE) of simulated water content for all individual scenarios ranges from 0.02 to 0.06  
 332 (Table 4). In general, the models reproduce well the water content and chloride concentrations. However, dynamic of measured  
 333 and simulated water contents differ considerably for ST1 and partly for ST2, although maximum values do match. The models  
 334 do not represent the high chloride concentrations in the uppermost part of soil profiles for ST3, WL1, and WL2. The standard  
 335 deviations in chloride concentration of the randomly selected model runs are exceptionally high in the lower part of ST2 that  
 336 corresponds to the poor sensitivity of the chloride concentration at the upper boundary and the comparably wide range of  
 337 measured chloride concentration in ponding water in the Salamat region ( $2.5 \text{ mg l}^{-1} - 25 \text{ mg l}^{-1}$ ).  
 338 The interannual variability of modelled groundwater recharge differs considerably among locations (Figure 6, Table 5). In  
 339 general, interannual groundwater recharge variability depends on vegetation and soil texture with related water retention  
 340 capacity. Vegetation with deep roots on soil with comparably high water retention capacity have a stronger interannual  
 341 variability, e.g. ST1, ST2 where recharge occurs only in years with high precipitation. Fine textured soils with shallow rooting  
 342 vegetation have an intermediate variability (WL1, WL2, and WL3), where years without recharge occur only during drought  
 343 periods. The coarser textured soils with grass cover has low interannual recharge variability (ST3) and recharge occurs each  
 344 year. Years with high precipitation, e.g. 2006, 2007, and 2008 in Waza Logone as well as 2010 in Salamat, produced strong  
 345 groundwater recharge.



The highest average annual recharge (93 mm) was calculated for ST3 in Salamat (Table 6), where water balance during the rainy season (July-September) is higher compared to the Waza Logone region and shallow rooting vegetation on comparably coarse soil texture with low water retention capacity and higher hydraulic conductivity prevail. The other locations in Salamat have lower calculated annual recharge, due to deep rooting vegetation and higher soil water retention capacity. The impact of soil texture on annual groundwater recharge becomes apparent by comparing the three location in Waza Logone with the same vegetation on soils with different water retention capacities and hydraulic conductivities. Groundwater recharge expressed as fraction of precipitation is between 1% and 4% (Table 5) and thus, within the range of 0.1 to 5% published by Scanlon et al. (2006). Only at WL2 (8%) and ST3 (12%), where coarse soil textures enhance recharge, a comparably high fraction is estimated.

Chloride concentration and water budget of the soils over the simulated time-period are rather unstable and differ for the six locations. At location ST2 with clay loam soil covered by Acacia and grass, accumulation of chloride takes place over several years, due to the high transpiration related to the effective field capacity (Figure 7). However, in high precipitation years, most of the accumulated chloride is leached to groundwater and soil concentration diminishes. It should be noted that at this site, the measured chloride concentrations cannot be reconstructed, if only input via precipitation is considered. The measured profile can only be plausibly modelled with an additional input via ponding water. Chloride input at the upper boundary is consequently six-times higher at ST2 compared to the other locations considered in this study.

At location ST3, the chloride accumulation is much lower compared to the other locations. Chloride budget is controlled by the fast groundwater recharge response to precipitation, which flushes chloride from the soil towards groundwater annually. The majority of chloride infiltrated with precipitation remains in the vadose zone over years and is leached towards groundwater mainly during years with precipitation or water infiltration above threshold values (Figure 7). Chloride accumulation is highest in profiles with clay soils and high effective field capacity (ST1, WL1, and WL3).

Chemical memory effects are subject to the dynamics of the water and chloride balance. Therefore, steady-state assumptions are unsuitable. Accurate estimations are only possible with transient assumptions.

#### 4.4 Evaporation and transpiration

The transpiration amount depends on the availability of water in the root zone and the type of vegetation cover. At ST1, annual transpiration presents two peaks: one related to sorghum and the other to grass (Figure 8). At each location and in every simulation year, soil water content in the root zone reaches the wilting point defined by the specific parametrization of the root water uptake model.

The actual evaporation rate depends mainly on the availability of water in the upper soil zone (Table 6). Clay and clay-loam with relatively high water storativity have larger amounts of evaporated water compared to sand and loam soils. During dry seasons, the uppermost part of the soils dries up annually, which restricts evaporation strongly.



Actual evapotranspiration is lower than the reference evapotranspiration most of the year. During and shortly after the rainy season, when sufficient soil water is available, actual evapotranspiration is comparable to or higher than  $ET_0$  depending on the vegetation.

## 5 Discussion

Soil texture information is helpful to limit possible MVG parameter ranges while searching for realistic parameter sets (Sprenger et al., 2015). However, poor representation of soil moisture dynamic using MVG parameters derived using Rosetta are reported (Sprenger et al., 2015) and indications are given that soil structure has to be taken into account (Vereecken et al., 2010), especially for soils where high rock content influences water flow due to inherent heterogeneity (Sprenger et al., 2015). The soils at the locations considered in this study belong to Quaternary sediments in the Lake Chad basin and heterogeneity, due to rock fragments is largely absent. Furthermore, soil moisture dynamics over the year are much higher in soils of the Waza Logone floodplain compared to soils from the more humid regions in the south, where precipitation, although large, occurs over 4-5 months and lacks over the rest of the year. It is expected that high soil moisture dynamics, rather homogeneous soils, and the monthly resolution of climate data result in minor impact of soil structure on MVG parametrization and groundwater recharge as shown in section 3.2. Soil moisture dynamics at all locations considered in this study are limited by water availability for evaporation in the uppermost part of the soil and by water uptake in the root zone, but not by the reference evapotranspiration. However, because time resolution of precipitation and evapotranspiration data is monthly, the models probably underestimate soil moisture dynamics.

Calculated chloride concentrations for the soil profiles give indications of appropriate MVG parametrization as well as evaporation and transpiration partitioning. However, uncertainty of chloride input and its transient variability in particular is expressed in rather wide and partly bimodal distribution of the scaling factor ( $sc\_Conc$ ) included in the calibration (Figures S1-S6 in supplement material). On one hand, measured chloride concentration in precipitation are in agreement with other studies in central Africa (Goni et al., 2001; Laouali et al., 2012; Gebru and Gebru and Tesfahunegn, 2019) and its transient behaviour within the rainy season is considered in the applied model. On the other hand, impact of dry deposition is unknown, because of data scarcity and potential lateral flow of periodical flooding. Furthermore, due to the monthly resolution of the atmospheric boundary condition, extreme rain events that cause surface runoff cannot be reflected in the model. The variability of chloride concentration in some of the soil profiles, which cannot be completely reproduced by the model, indicates either a higher variability of chloride input and/or a larger variability in soil physics.

Bouchez et al. (2019) identified a chloride deficit between deposition and river export in the Chari-Logone river system of 88% (only 12% of the deposited chloride is exported via river water). They refer to the chemical memory effect, which can play an important role in arid regions. Our simulations show the importance of the vadose zone for storage of chloride over longer periods of time, which explains the fate of chloride in the basin and confirms the chemical memory effect. In this context, it must be noted that the thickness of the vadose zone at the locations considered in this study is between 4 m and 21



409 m, where important amounts of chloride can be potentially stored leading to a strong delay of the chemical signal from  
 410 precipitation to groundwater.

411 In general, the calculated mean annual groundwater recharge values are within the ranges of 0.2 to 35 mm yr<sup>-1</sup> estimated by  
 412 Edmunds et al. (2002) using the CMB method in seven chloride profiles in northern Nigeria. The larger values (90 mm yr<sup>-1</sup> in  
 413 ST3 and 54 mm yr<sup>-1</sup> in WL2) are due to local coarse soil.

## 414 6 Conclusions

415 The quantitative estimation of groundwater recharge in the LCB is difficult, due to the scarce data availability and the expected  
 416 low recharge quantities. Estimation of low recharge amounts in arid and semi-arid areas are usually ambiguous, because the  
 417 immanent measurement inaccuracies lead to uncertainties during data processing and modelling. Quantification of water and  
 418 solute fluxes in the vadose zone is often implemented using long-term time series of soil moisture, pressure heads, and  
 419 concentration data in combination with appropriate models. Monitoring of soil moisture and solute concentration over longer  
 420 periods at different depths and sites is difficult in the LCB, due to limited infrastructural prerequisites and challenging climatic  
 421 boundary conditions. The presented approach combines soil moisture and chloride concentration quantified along vertical soil  
 422 profiles in different locations within the LCB with numerical models and freely accessible data, while considering data  
 423 uncertainty. Calculated chloride concentrations for the soil profiles give indications of appropriate MVG parametrization as  
 424 well as evaporation and transpiration partitioning. Although dynamic of measured and simulated for both water contents and  
 425 chloride concentration differ considerably in profiles ST1 and partly ST2, their magnitudes agree largely. This is especially  
 426 important for chloride concentration in the middle and deeper parts of the profiles, where seasonal effects are mainly averaged.  
 427 Thus, the estimates of soil water balance and especially of groundwater recharge as well as the adopted soil physical parameters  
 428 are plausible.

429 Mean groundwater recharge values estimated in this study are different to those published in Tewolde et al. (2019). This is  
 430 due to the more extensive availability of chloride concentration data in precipitation for this study. In addition, Tewolde et al.  
 431 (2019) roughly estimated one value of saturated porosity for each profile. This parameter is rather sensitive in the Bayesian  
 432 calibration and several values along each of the profiles were considered in this study. In contrast to the assessment of  
 433 groundwater recharge with the CMB (Tewolde et al., 2019), the method used here allows not only estimates of mean recharge,  
 434 but also its interannual dynamics, variability, and the classification of the uncertainties of the input data and modelling results.  
 435 The interannual variability of groundwater recharge is generally higher than the uncertainty of the modelled groundwater  
 436 recharge. The soil moisture dynamics at all locations considered in this study are limited by water availability for evaporation  
 437 in the uppermost part of the soil and by water uptake in the root zone and not by the reference evapotranspiration.

438 Simulations show the importance of the vadose zone for storage of chloride over longer time-periods and explain the fate of  
 439 chloride in the basin. The thickness of the vadose zone at the locations considered in this study varies between 4 m and 21 m.  
 440 Important amounts of chloride can be potentially stored delaying strongly the chemical signal from precipitation to  
 441 groundwater.



Upscaling of the results to larger areas must be interpreted with caution since the considered combinations of soils and vegetation probably do not cover all combinations present in Salamat and Waza Logone regions.

#### Author contribution

M.R. conducted fieldwork; A.G.M.S. and C.N. conducted modelling and interpretation; C.N. and S.V. design the study and conducted writing. All authors contributed to the discussion of results and commented on the manuscript.

#### Acknowledgement

This study was conducted within the framework of the technical cooperation project “Lake Chad Basin - Management of Groundwater Resources” jointly executed by the Lake Chad Basin Commission (LCBC) and the German Federal Institute for Geosciences and Natural Resources (BGR). The technical project is funded by the German Federal Ministry for Economic Cooperation and Development (BMZ). We thank Daniel Tewolde, Paul Königer and Anna Degtjarev for their support in the lab.

#### References

- Allen, R. G., Pereira, L. S., Dirk, R., and Smith, M.: Crop evapotranspiration: Guidelines for computing crop water requirements. FAO Irrigation and Drainage Paper No. 56. Rome, Italy. <https://doi.org/10.1016/j.eja.2010.12.001>, 1998.
- Alves, M. E. B., Mantovani, E. C., Sedyama, G. C., & Neves, J. C. L. (2013). Estimate of the crop coefficient for Eucalyptus cultivated under irrigation during initial growth. *Cerne*, 19(2), 247–253. <https://doi.org/10.1590/s0104-77602013000200008>
- Anderson, R. G., Zhang, X., and Skaggs, T. H.: Measurement and Partitioning of Evapotranspiration for Application to Vadose Zone Studies. *Vadose Zone Journal*, 16(13), 0. <https://doi.org/10.2136/vzj2017.08.0155>, 2017
- Aouade, G., Ezzahar, J., Amenouz, N., Er-Raki, S., Benkaddour, A., Khabba, S., and Jarlan, L.: Combining stable isotopes, Eddy Covariance system and meteorological measurements for partitioning evapotranspiration, of winter wheat, into soil evaporation and plant transpiration in a semi-arid region. *Agricultural Water Management*, 177, 181–192. <https://doi.org/10.1016/J.AGWAT.2016.07.021>, 2016.
- Bader, J., Lemoalle, J., and Leblanc, M.: Modèle hydrologique du Lac Tchad, *Hydrolog. Sci. J.*, 56, 411–425, 2011.
- Batello, C., Marzot, M., and Harouna Touré, A.: The future is an ancient lake: Traditional knowledge, biodiversity and genetic resources for food and agriculture in the Lake Chad basin ecosystems. FAO Interdepartmental Working Group on Biological Diversity for Food and Agriculture, Rome, 2004.
- Bernacsek, G. M., Hughes, J. S., and Hughes, R. H. (Ed.): A directory of African wetlands. International Union for the Conservation of Nature and Natural Resources, 1992.
- Beyer, M., Koeniger, P., and Himmelsbach, T.: Constraining water uptake depths in semi-arid environments using stable water isotopes Results & Discussion. <https://doi.org/10.5281/zenodo.56159>, 2016.



- 472 Bouchez, C., Deschamps P., Goncalves J., Hamelin B., Nour AM, Vallet-Coulomb C & Sylvestre F: Water transit time and  
 473 active recharge in the Sahel inferred by bomb-produced  $^{36}\text{Cl}$ . *Nature, scientific reports*, 9: 7465, (2019).
- 474 Bouchez, C., Goncalves, J., Deschamps, P., Vallet-Coulomb, C., Hamelin, B., Doumnang, J.C., Sylvestre, F.: Hydrological,  
 475 chemical, and isotopic budgets of Lake Chad: a quantitative assessment of evaporation, transpiration and infiltration fluxes,  
 476 *Hydrol. Earth Syst. Sci.*, 20, 1599–1619, 2016.
- 477 Carmouze, J.-P.: Originalité de la régulation saline du lac Tchad, *Comptes Rendus de l'Académie des Sciences. Série D:*  
 478 *Sciences Naturelles*, 275, 1871–1874, 1972.
- 479 Cuthbert, M. O., Taylor, R.G., Favreau, G. et al.: Observed controls on resilience of groundwater to climate variability in sub-  
 480 Saharan Africa. *Nature*, 572: 230–234, <https://doi.org/10.1038/s41586-019-1441-7>, 2019.
- 481 Didan, K.: MOD13Q1 MODIS/Terra Vegetation Indices 16-Day L3 Global 250m SIN Grid V006. NASA EOSDIS Land  
 482 Processes DAAC. <https://doi.org/10.5067/MODIS/MOD13Q1.006>, 2015.
- 483 Didane, D. H., Rosly, N., Zulkafli, M. F., and Shamsudin, S. S.: Evaluation of wind energy potential as a power generation  
 484 source in Chad. *International Journal of Rotating Machinery*, vol. 2017, Article ID 3121875, 10 pp, 2017.
- 485 Do, F. and Rocheteau, A.: Cycle annuel de transpiration d'Acacia raddiana par la mesure des flux de sève brute (Nord-Sénégal).  
 486 In *Un arbre au désert: Acacia raddiana* (pp. 119–142). Paris, (2003).
- 487 Do, F. C., Rocheteau, A., Diagne, A. L., Goudiaby, V., Granier, A., and Lhomme, J. P.: Stable annual pattern of water use by  
 488 *Acacia tortilis* in Sahelian Africa. *Tree Physiology*, 28(1), 95–104. <https://doi.org/10.1093/treephys/28.1.95>, 2008.
- 489 Edmunds, W. M. and Gaye, C.B.: Estimating the spatial variability of groundwater recharge in the Sahel using chloride. *J.*  
 490 *Hydrol.*, 156(1-4):47-59, 1994.
- 491 Edmunds, W. M., Fellman, E., and Goni, I. B.: Spatial and temporal distribution of groundwater recharge in northern Nigeria.  
 492 *Hydrogeology Journal*, 10:205-215, 2002.
- 493 Feddes, R. A., Kowalik, P. J., and Zaradny, H.: Simulation of field water use and crop yield. Published in 1978 in Wageningen  
 494 by Centre for agricultural publishing and documentation. Wageningen: Centre for Agricultural Pub. and Documentation.  
 495 <https://lib.ugent.be/catalog/rug01:000032129>, 1978.
- 496 Fontes, J.-C., Maglione, G., and Roche, M.-A.: Données isotopiques préliminaires sur les rapports du lac Tchad avec les nappes  
 497 de la bordure nord-est, *Cah. Orstom. Hydrobiol.*, 6, 17– 34, 1969.
- 498 Fontes, J.-C., Gonfiantini, R., and Roche, M.-A. : Deuterium et oxygène-18 dans les eaux du Lac Tchad. *Isotope Hydrology*,  
 499 *IAEA-SM-129/23*, 1970.
- 500 Gebru, T.A. and Tesfahunegn, G.B.: Chloride mass balance for estimation of groundwater recharge in a semi-arid catchment  
 501 of northern Ethiopia. *Hydrogeology Journal*, 27:363-378, 2019.
- 502 Global Soil Data Task Group: Global Gridded Surfaces of Selected Soil Characteristics (IGBP-DIS). ORNL DAAC, Oak  
 503 Ridge, Tennessee, USA. <https://doi.org/10.3334/ORNLDAAAC/569>, 2000.
- 504 Goni, I., Fellman, E., and Edmunds, W.: Rainfall geochemistry in the Sahel region of northern Nigeria, *Atmos. Environ.*, 35,  
 505 4331– 4339, 2001.



- 506 Groh, J., Stumpp, C., Lücke, A., Pütz, T., Vanderborght, J., and Vereecken, H.: Inverse estimation of soil hydraulic and  
 507 transport parameters of layered soils from water stable isotopes and lysimeter data, *Vadose Zone Journal* 17:170168.  
 508 Doi:10.2136/vzj2017.09.0168, 2018.
- 509 Gröning, M., Lutz, H.O., Roller-Lutz, Z., Kralik, M., Gourcy, L., Pölsenstein, L.: A simple rain collector preventing water re-  
 510 evaporation dedicated for  $\delta^{18}\text{O}$  and  $\delta^2\text{H}$  analysis of cumulative precipitation samples. *J. Hydrol.* 448-449, 195-200, 2012.
- 511 Harris, I., Osborn, T. J., Jones, P. and Lister, D.: Version 4 of the CRU TS monthly high-resolution gridded multivariate  
 512 climate dataset. *Sci Data* 7, 109 (2020) <https://doi.org/10.1038/s41597-020-0453-3>.
- 513 Isihoro, S., Matisoff, G., and Wehn, K.: Seepage relationship between Lake Chad and the Chad Aquifers, *Groundwater*, 34,  
 514 819–826, 1996.
- 515 Hartig, F., Minunno, F., Paul, S.: *BayesianTools: General-Purpose MCMC and SMC Samplers and Tools for Bayesian*  
 516 *Statistics*, 2019.
- 517 Jasechko, S., Sharp, Z. D., Gibson, J. J., Birks, S. J., Yi, Y., and Fawcett, P. J.: Terrestrial water fluxes dominated by  
 518 transpiration, *Nature*, 496, 347–350, 2013.
- 519 Kool, D., Agam, N., Lazarovitch, N., Heitman, J. L., Sauer, T. J., and Ben-Gal, A.: A review of approaches for  
 520 evapotranspiration partitioning. *Agricultural and Forest Meteorology*, 184, 56–70, 2014.
- 521 Lake Chad Basin Commission. (1993). Monitoring and management of groundwater resources in the Lake Chad Basin.  
 522 Mapping of aquifers, water resources management, final report, R35985, Report BRGM R 35985 EA U/4S/93.
- 523 Lake Chad Basin Commission. (2012). Report on the State of the Lake Chad Basin Ecosystem.  
 524 [http://www.cbtl.org/sites/default/files/download\\_documents/report\\_on\\_the\\_state\\_of\\_the\\_lake\\_chad\\_basin\\_ecosystem.pdf](http://www.cbtl.org/sites/default/files/download_documents/report_on_the_state_of_the_lake_chad_basin_ecosystem.pdf).
- 525 Laouali, D., Galy-Lacaux, C., Diop, B., Delon, C., Orange, D., Lacaux, J.P., Akpo, A., Lavenu, F., Gardrat, E., Castera, P.,  
 526 2012. Long term monitoring of the chemical composition of precipitation and wet deposition fluxes over three Sahelian  
 527 savannas. *Atmos. Environ.* 50, 314–327. <https://doi.org/10.1016/j.atmosenv.2011.12.004>
- 528 Leblanc, M.: Gestion des ressources en eau des grands bassins semi-arides à l'aide de la télédétection et des SIG: application  
 529 à l'étude du bassin du lac Tchad, Afrique, PhD thesis, Université de Poitiers, Poitiers, 2002.
- 530 Leblanc, M., Favreau, G., Tweed, S., Leduc, C., Razack, M., and Mofor, I.: Remote sensing for groundwater modelling in  
 531 large semiarid areas: Lake Chad basin, Africa. *Hydrogeology Journal*, 15(1), 97-100, 2007.
- 532 Lemoalle, J., Bader, J.-C., Leblanc, M., and Sedick, A.: Recent changes in Lake Chad: observations, simulations and  
 533 management options (1973–2011), *Global Planet. Change*, 80, 247–254, 2012.
- 534 Lloyd, J. W.: A review of aridity and groundwater, *Hydrological Processes*, Vol. 1, 63-78, 1986.
- 535 Lloyd, J. W.: Groundwater in arid and semiarid regions. In: Silveira, L. and Usunoff E.J. [Eds.]: *Groundwater* (Vol. I),  
 536 *Encyclopedia of Life Support Systems*, pp. 284–307, 2009.
- 537 Majnooni-Heris, A., Sadraddini, A. A., Nazemi, A. H., Shakiba, M. R., Neyshaburi, M. R., and Tuzel, I. H.: Determination of  
 538 single and dual crop coefficients and ratio of transpiration to evapotranspiration for canola. *Annals of Biological Research*,  
 539 3(4), 1885–1894, 2012.



- 540 Mertens, J., Barkle, G. F., and Stenger, R.: Numerical analysis to investigate the effects of the design and installation of  
541 equilibrium tension plate lysimeters on leachate volume, *Vadose Zone Journal*, 4:488-499, 2005.
- 542 Millington, R. J. and Quirk, J. P.: Permeability of porous solids. *Trans. Int. Congr. Soil Sci.*, 7(1), 97-106, 1961.
- 543 Mualem, Y.: A new model for predicting the hydraulic conductivity of unsaturated porous media, *Water Resour. Res.*, 12,  
544 513–522, doi:10.1029/WR012i003p00513, 1976.
- 545 Ngatcha, B. N., Mudry, J., and Leduc, C.: The state of understanding on groundwater recharge for the sustainable management  
546 of transboundary aquifer in the Lake Chad basin, 2008.
- 547 Olivry, J., Chouret, A., Vuillaume, G., Lemoalle, J., and Bricquet, J.: *Hydrologie du lac Tchad*, Editions de l'ORSTOM, Paris  
548 1996.
- 549 Richards, L. A.: Capillary conduction of liquids through porous mediums. *Physics*, 1(5), 318-333, 1931.
- 550 Righes, A. A.: Water uptake and root distribution of soybeans, grain sorghum and corn. *Retrospective Theses and*  
551 *Dissertations*. Iowa State University, 1980.
- 552 Roche, M.: *Tracage naturel salin et isotopique des eaux du système du Lac Tchad*, These de Doctorat d'Etat, Travaux et  
553 Documents de l'ORSTOM, ORSTOM (Office de la Recherche Scientifique et Technique d'Outre-Mer) editions, Paris, 1980.
- 554 Scanlon, B. R., Keese, K. E., Flint, A. L., Flint, L. E., Gaye, C. B., Edmunds, W. M., and Simmers, I.: Global synthesis of  
555 groundwater recharge in semiarid and arid regions. *Hydrol. Process.* 20, 3335-3370, 2006.
- 556 Schaap, M. G., Leij, F. J., and van Genuchten, M. T.: ROSETTA: a computer program for estimating soil hydraulic parameters  
557 with hierarchical pedotransfer functions, *Journal of Hydrology*, 251, 163-176, 2001.
- 558 Schenk, H. J. and Jackson, R. B.: Rooting depths, lateral root spreads and belowground aboveground allometries of plants in  
559 water limited ecosystems. *Journal of Ecology*, 90, 480–494. <https://doi.org/10.1046/j.1365-2745.2002.00682.x>, 2002.
- 560 Shahrokhnia, M. H. and Sepaskhah, A. R.: Single and dual crop coefficients and crop evapotranspiration for wheat and maize  
561 in a semi-arid region. *Theoretical and Applied Climatology*, 114(3–4), 495–510. <https://doi.org/10.1007/s00704-013-0848-6>,  
562 2013.
- 563 Šimůnek, J., Sejna, M., Saito, H., Sakai, M., and van Genuchten, M. Th.: *The HYDRUS-1D software package for simulating*  
564 *the one-dimensional movement of water, heat, and multiple solutes in variably-saturated media*, Version 4.15, Riverside,  
565 California, 2009.
- 566 Šimůnek, J., Šejna, M., & van Genuchten, M. T.: *The HYDRUS Software Package for Simulating the Two- and Three-*  
567 *Dimensional Movement of Water, Heat, and Multiple Solutes in Variably-Saturated Media*. Prague, 2011.
- 568 Sprenger, M., Volkmann, T. H. M., Blume, T., and Weiler, M.: Estimating flow and transport parameters in the unsaturated  
569 zone with pore water stable isotopes, *Hydrol. Earth Syst. Sci.*, 19(6), 2617-2635, doi:10.5197/hess-19-2617-2015, 2015.
- 570 Stumpp, C., Nützmann, G., Maciejewski, S., and Maloszewski, P.: A comparative modeling study of a dual tracer experiment  
571 in a large lysimeter under atmospheric conditions, *Journal of Hydrology*, 375, 566-577, 2009.

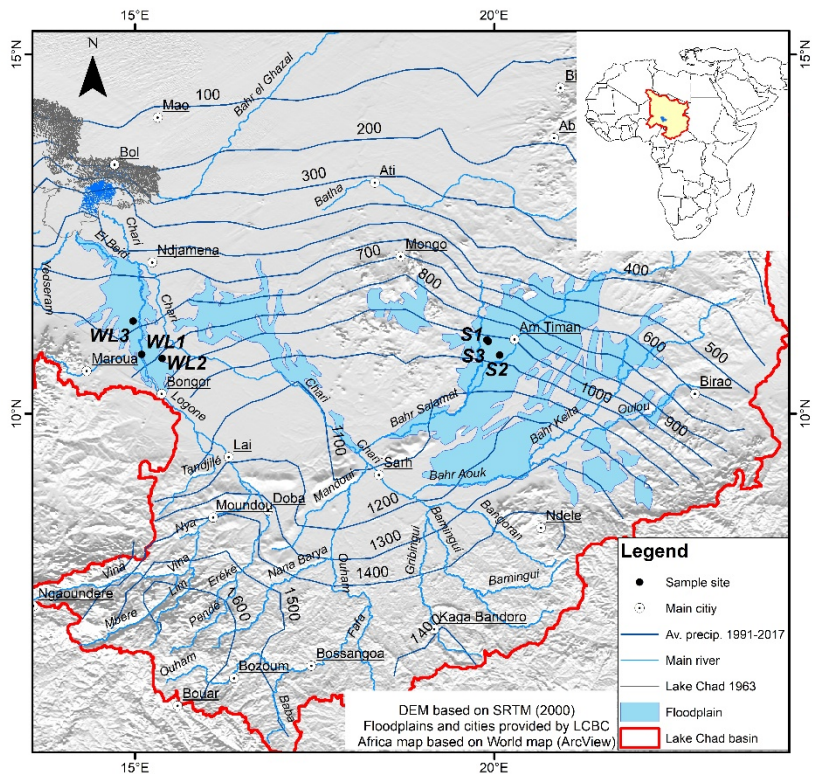


- 572 Stumpp, C., Stichler, W., Kandolf, M., and Šimůnek, J.: Effects of land cover and fertilization method on water flow and solute  
573 transport in five lysimeters: a long-term study using stable water isotopes, *Vadose Zone Journal*, 11(1), doi:  
574 10.2136/vzj2012.0075, 2012.
- 575 ter Braak, C.J.F., Vrugt, J.A.: Differential Evolution Markov Chain with snooker updater and fewer chains. *Stat. Comput.* 18,  
576 435–446. <https://doi.org/10.1007/s11222-008-9104-9>, 2008.
- 577 Tewolde, D. O.: Investigating unsaturated zone water transport processes by means of biogeochemical analysis of soil depth  
578 profiles: a comparative study of two semi-arid sites. M.Sc.-Thesis, Leibniz Universitaet Hannover, 2017.
- 579 Tewolde, D. O., Koeniger, P., Beyer, M., Neukum, C., Gröschke, M., Ronnelngar, M., Rieckh, H., and Vassolo, S.: Soil water  
580 balance in the Lake Chad Basin using stable water isotope and chloride of soil profiles. *Isot. Environ. Health Stud.* 55, 459-  
581 477. <https://doi.org/10.1080/10256016.2019.1647194>, 2019.
- 582 Tong, G. D., Liu, H. L., and Li, F. H.: Evaluation of dual crop coefficient approach on evapotranspiration calculation of cherry  
583 trees. *International Journal of Agricultural and Biological Engineering*, 9(3), 29–39.  
584 <https://doi.org/10.3965/j.ijabe.20160903.1886>, 2016.
- 585 Vanderborght, J. and Vereecken, H.: Review of dispersivity for transport modeling in soils, *Vadose Zone Journal*, 6(1), 29-52,  
586 doi:10.2136/vzj2006.0096, 2007.
- 587 van Genuchten, M. T.: A close-form equation for predicting the hydraulic conductivity of unsaturated soils 1, *Soil Science*  
588 *Society of America Journal*, 8(44), 892-898, 1980.
- 589 van Looy, K., Bouma, J., Herbst, M., Koestel, J., Minasny, B., Mishra, U., Montzka, C., Nemes, A., Pachepsky, Y. A.,  
590 Padarian, J., and Schaap, M. G.: Pedotransfer functions in earth system science: challenges and perspectives, *Reviews of*  
591 *Geophysics*, 55(4), 1199-1256, doi: 10.1002/2017RG000581, 2017.
- 592 Vassolo, S.: The aquifer recharge and storage systems to reduce the high level of evapotranspiration. In: *Adaptive Water*  
593 *Management in the Lake Chad Basin*. World Water Week 09, FAO, pp. 30-44, 2009.
- 594 Vereecken, H., Javaux, M., Weynants, M., Pachepsky, Y. A., Schaap, M. G., and van Genuchten M. T.: Using pedotransfer  
595 functions to estimate the van Genuchten-Mualem soil hydraulic properties: A review, *Vadose zone Journal*, 9(4), 759-820,  
596 doi: 10.2136/vzj2010.0045, 2010.
- 597 Vereecken, H., Schnepf, A., Hopmans, J. W., Javaux, M., Or, D., Roose, T., ... and Young, I. M.: Modeling soil processes:  
598 Review, key challenges, and new perspectives, *Vadose Zone Journal*, 15(5), 1-57, doi: 10.2136/vzj.2015.09.0131, 2016.
- 599 Vieira, P. V. D., de Freitas, P. S. L., Ribeiro da Silva, A. L. B., Hashiguti, H. T., Rezende, R. and Junior, C. A. F.: Determination  
600 of wheat crop coefficient (Kc) and soil water evaporation (Ke) in Maringa, PR, Brazil, *African Journal of Agricultural*, 11(44),  
601 4551–4558. <https://doi.org/10.5897/AJAR2016.11377>, 2016.
- 602 Vuillaume, G.: Bilan hydrologique mensuel et modélisation sommaire du régime hydrologique du lac Tchad, *Cahiers*  
603 *ORSTOM. Série Hydrologie*, 18, 23–72, 1981.
- 604 Wu, Y., Du, T., Ding, R., Tong, L., and Li, S.: Multiple Methods to Partition Evapotranspiration in a Maize Field. *Journal of*  
605 *Hydrometeorology*, 139–149. <https://doi.org/10.1175/JHM-D-16-0138.1>, 2016.



606 Zairi, R.: Étude géochimique et hydrodynamique du Bassin du Lac Tchad (la nappe phréatique dans les régions du Kadzell  
607 (Niger oriental) et du Bornou (Nord-Est du Nigéria)), PhD thesis, Université de Montpellier 2, Montpellier, 2008.  
608

609  
610 **Figure 1: Location of the six soil sampling sites within the Logone and Salamat river basins in the Lake Chad catchment. The map**  
611 **inlet shows the location of the Lake Chad basin in Africa.**



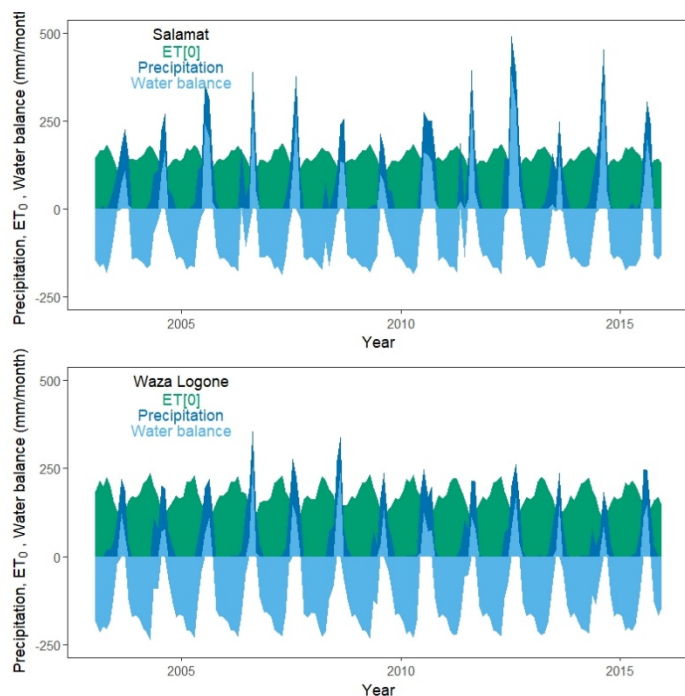


**Figure 2: Monthly precipitation, reference evapotranspiration from the CRUTS 4 database (NCAR, 2017) and derived water balance for Salamat and Waza Logone.**

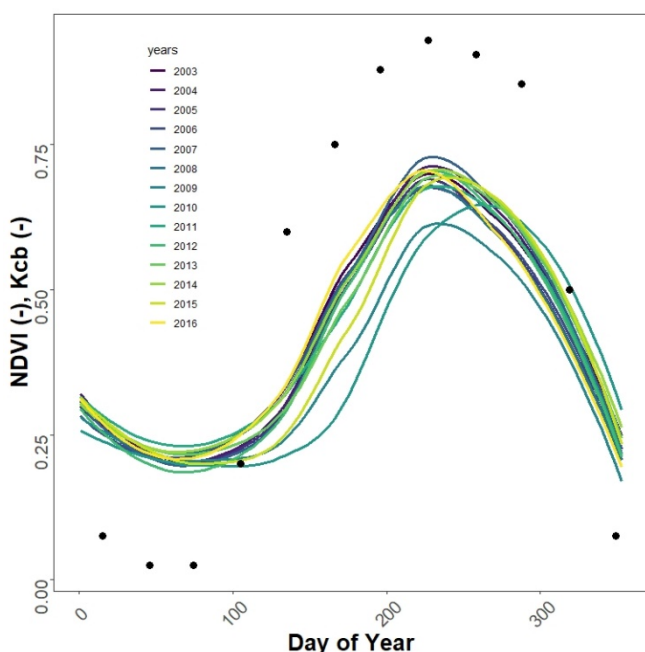


**Figure 3: Average Normalized Difference Vegetation Index (NDVI, MODIS 16 day interval and 250 m spatial resolution) measured between 2003 and 2016 in the Salamat region and estimated monthly basal crop coefficient (Kcb, black points) for location S3.**

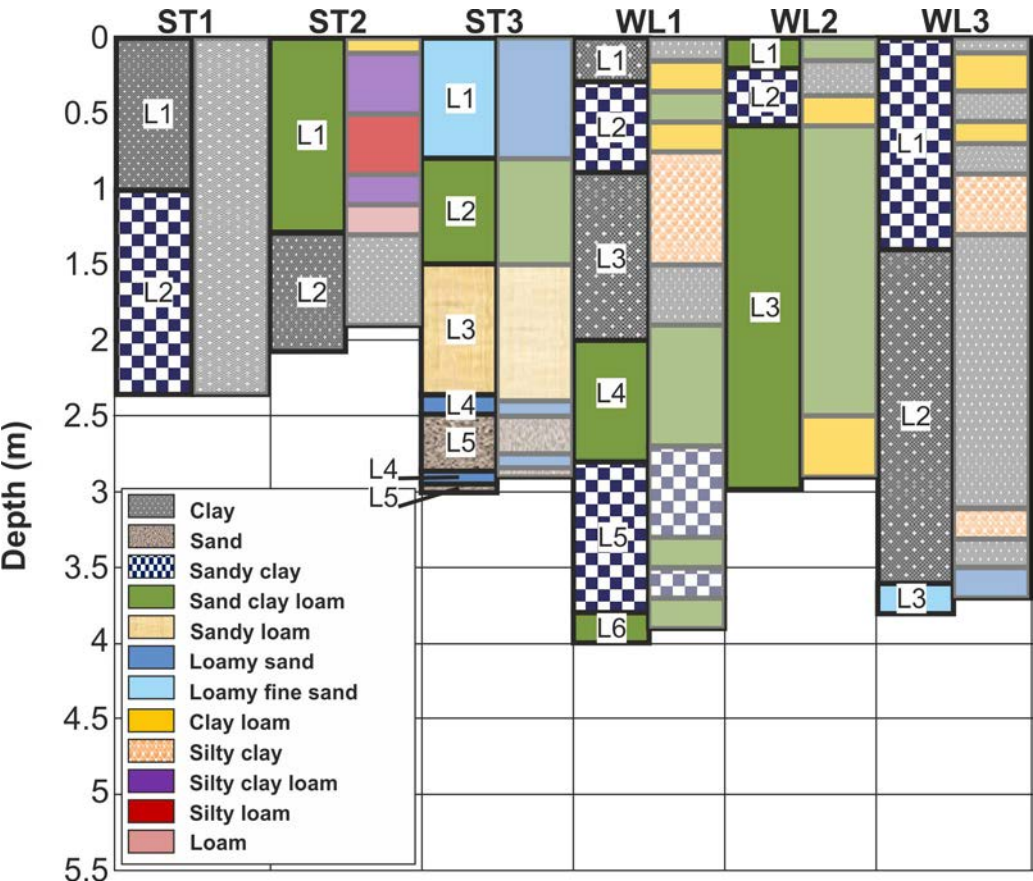
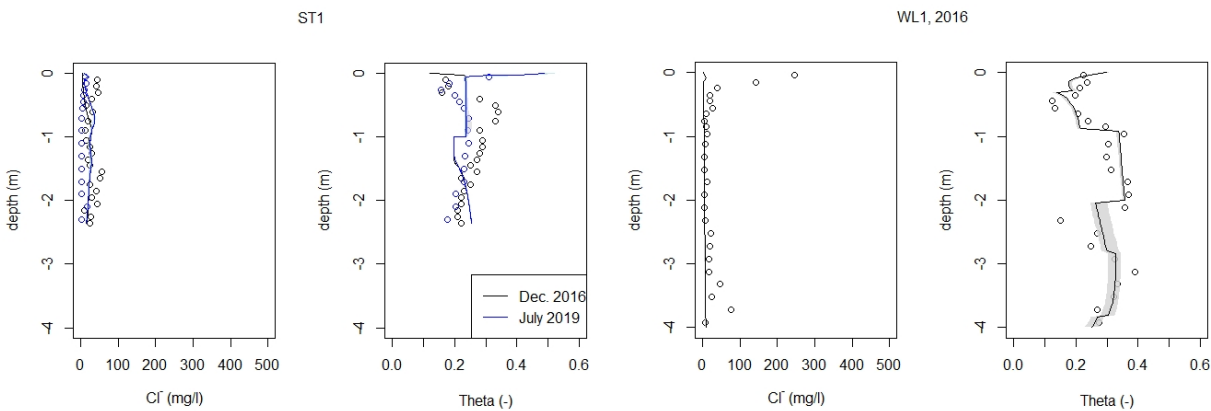
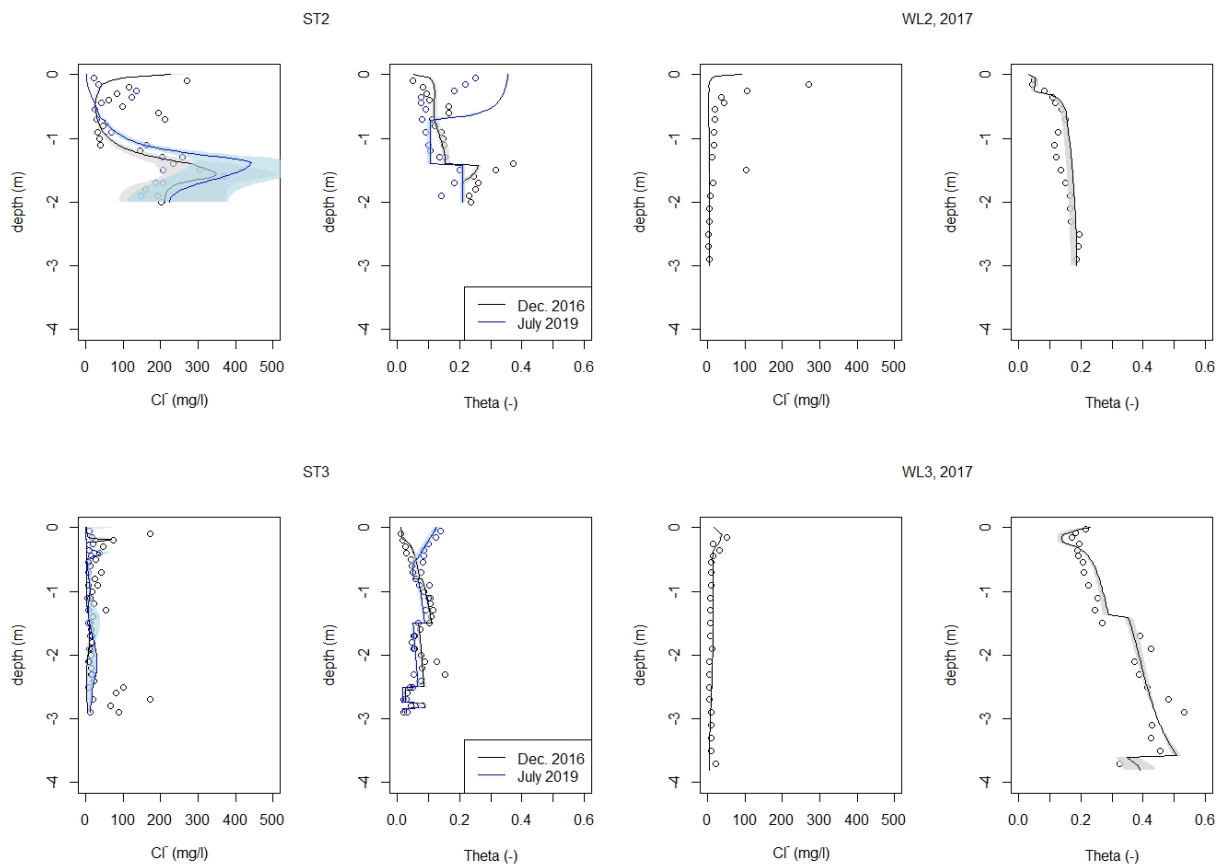
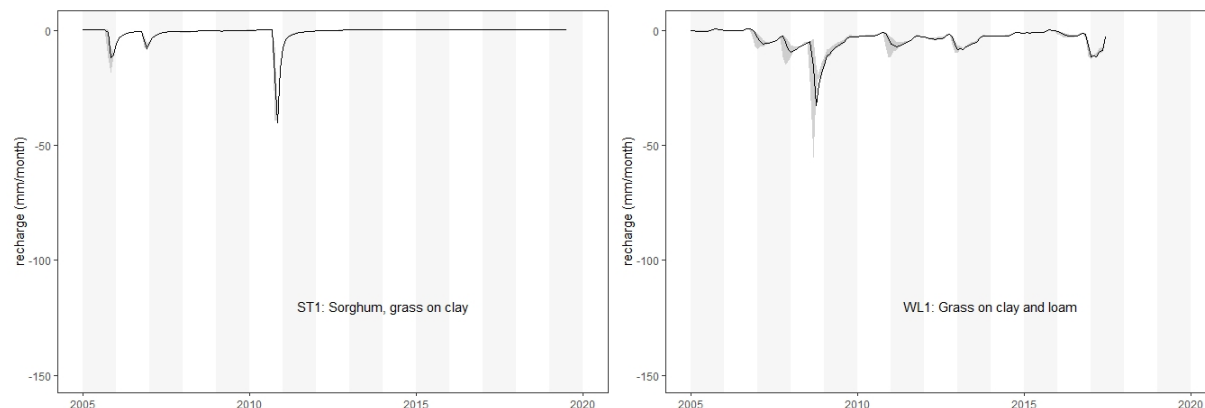


Figure 4: Soil textures used in the model (left column) defined according to the grain size distribution analysis (right column) for each of the six soil profiles.





**Figure 5: Measured and simulated scenarios of chloride concentration and water content for all six soil profiles. Shaded areas represent standard deviation of 100 randomly selected model runs.**



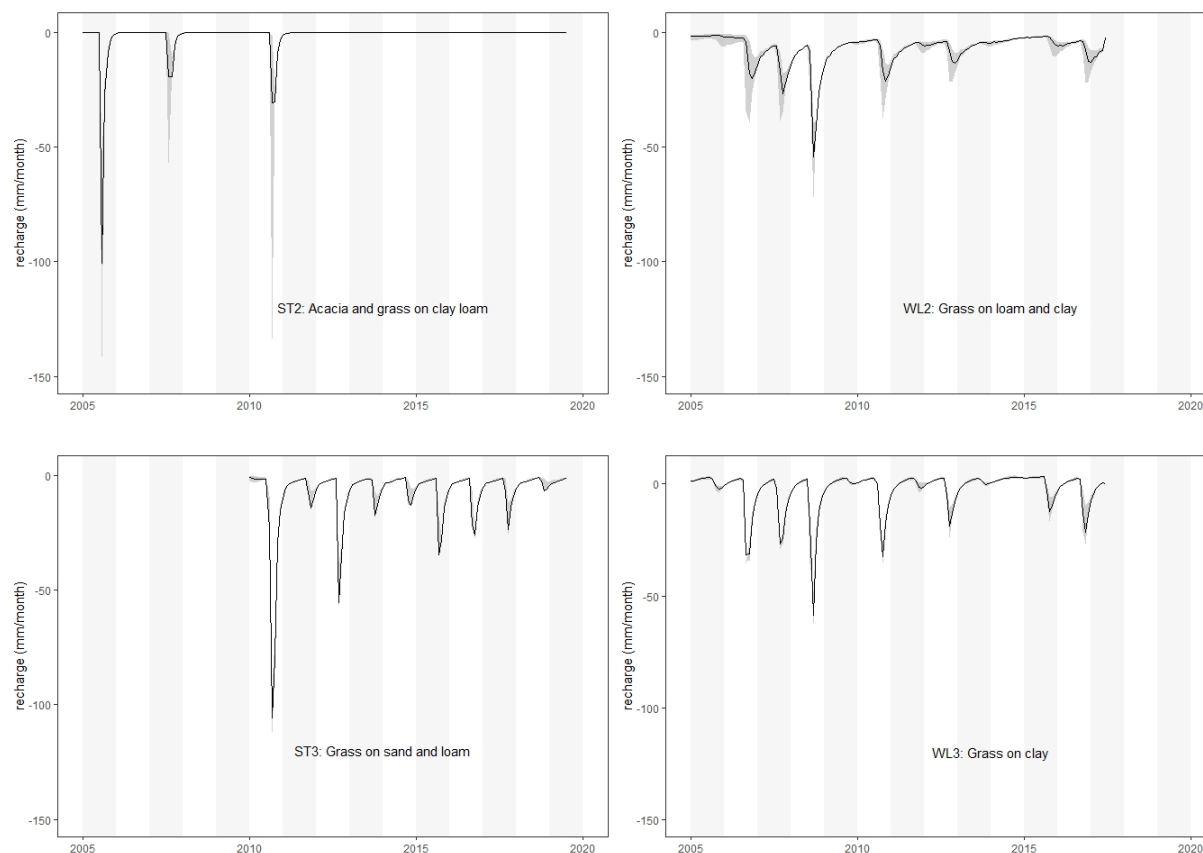


**Figure 6: Calculated groundwater recharge for all scenarios and sampling locations with indication of vegetation and soil texture.**

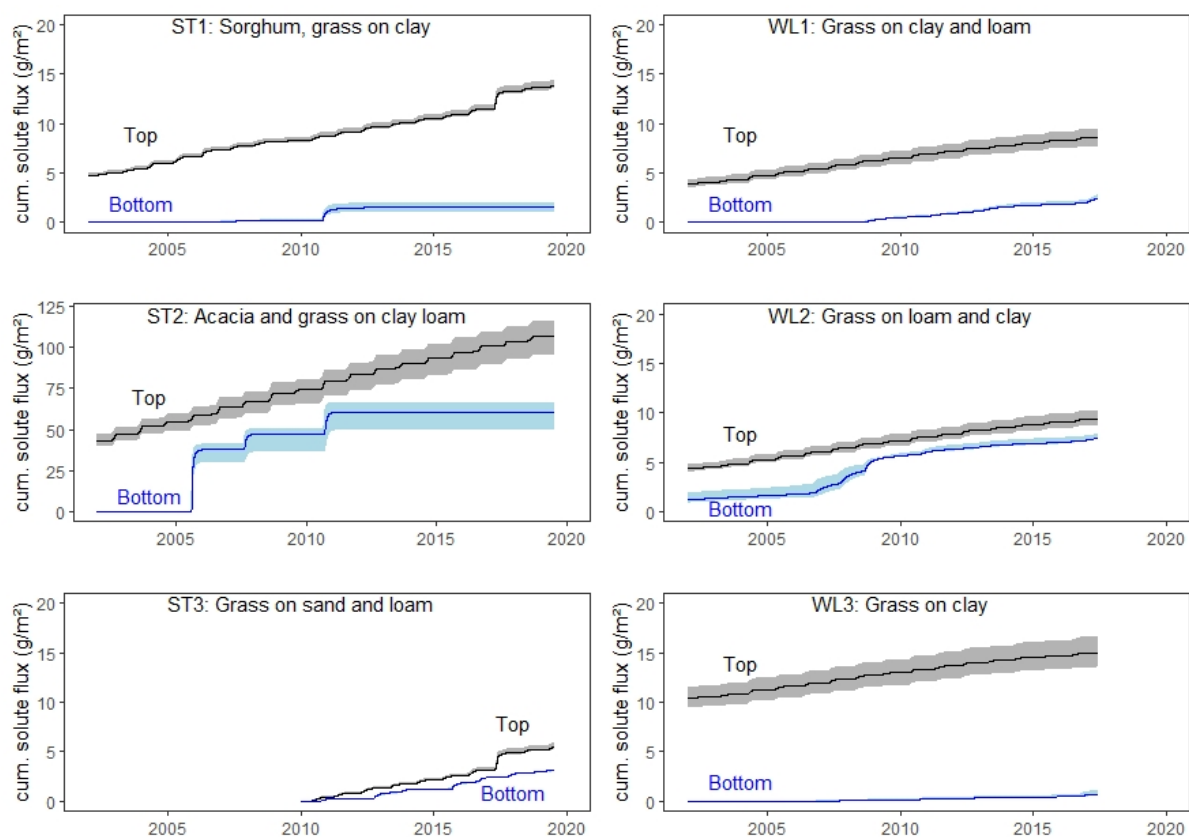


**Fig. 7: Cumulative solute flux on the upper and lower boundary of the models. The shaded areas represents the standard deviation of 100 randomly selected model runs. Note the different y-axis scales between sites.**

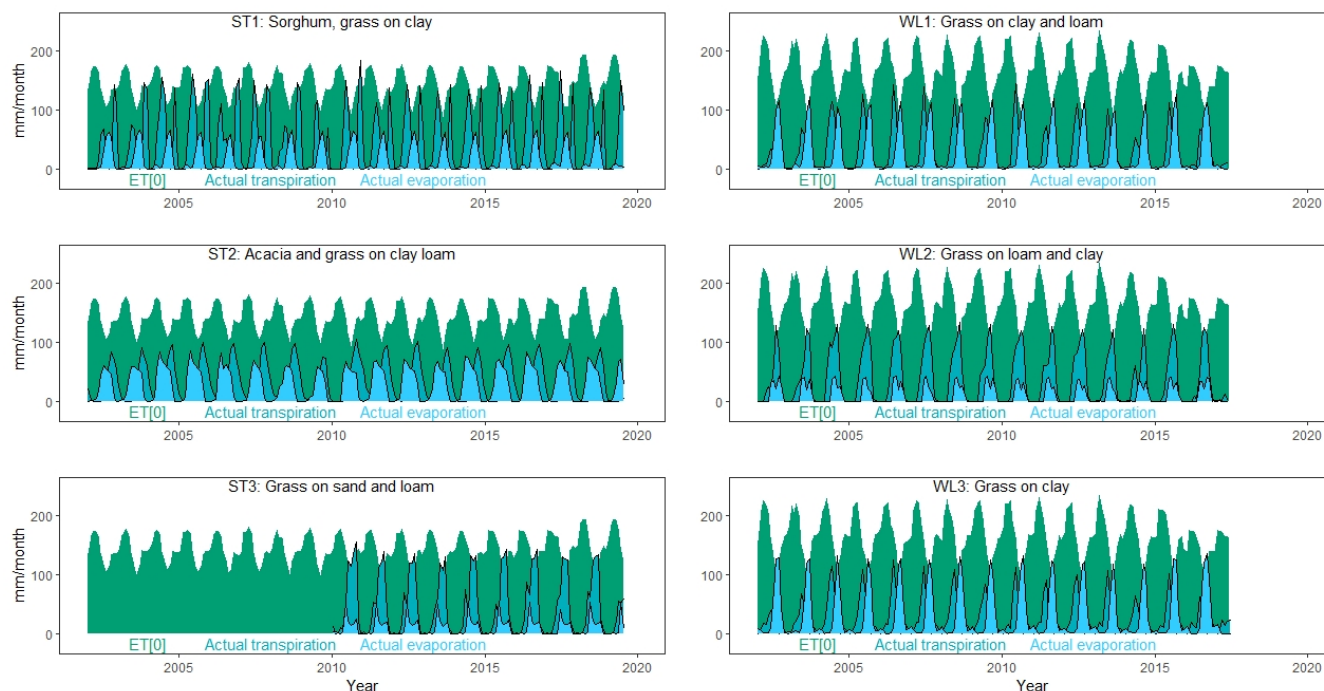


**Fig. 8: Reference evapotranspiration from the CRUTS 4 database (NCAR 2017) as well as modelled average actual evaporation and transpiration of 100 randomly selected model runs.**

**Table 1: Names and geographic coordinates of the sampling locations with indication of average depth to groundwater.**

Name	Location	Date of Sampling	Drilling depth (m)	Longitude (°)	Latitude (°)	Elevation (m a.s.l.)	Depth to Groundwater (m)
ST1	Gos	07-12-2016	2.35	19.89644	11.02582	418	21
	Djarat	11-07-2019	5.0				
ST2	Kach	09-12-2016	2.0	20.07473	10.81649	396	16-18
	Kacha	16-07-2019	5.0				
ST3	Gos	11-12-2016	2.2	19.91687	11.00629	418	21
	Djarat	13-07-2019	5.0				
WL1	Katoa	01-06-2017	4.0	15.09235	10.82508	362	4
WL2	Loutou	01-06-2017	3.0	15.37817	10.76805	325	11-12
WL3	Zina	08-06-2017	3.8	14.97363	11.28858	304	3.6



642 **Table 2: Crop evapotranspiration scenario used with the individual soil profiles.**

Scenario	Kcb	Ke	Root depth	Profile
Mean	average	average	average	All profiles
Min	minimum	minimum	average	All profiles
Min-RD	minimum	minimum	minimum	WL1
Mix-1	minimum	average	average	All profiles
Mix-2	average	minimum	average	ST1, WL2, WL3
Mix-3	maximum	average	average	ST3
Max	maximum	maximum	average	All profiles

643

644 **Table 3: Parametrization of water retention and unsaturated hydraulic conductivity functions according the Mualem-van**  
 645 **Genuchten model after Bayesian model calibration.**

Location	Texture	Depth (m)	$\theta_r$ (-)	$\theta_s$ (-)	$\alpha$ (m <sup>-1</sup> )	n (-)	K <sub>s</sub> (md <sup>-1</sup> )
ST1	Clay	0-1	0.001	0.61±0.01	2.13±0.27	1.164±0.008	0.09±0.14
	Sandy clay	1-2.35	0.04	0.43±0.03	2.63±0.37	1.150±0.011	0.43±0.39
ST2	Sandy clay loam	0-1.4	0.04	0.38±0.02	1.18±0.08	1.36±0.047	0.03±0.16
	Clay	1.4 -2.1	0.07	0.48±0.08	2.66±0.36	1.203±0.052	0.11±0.28
ST3	Loamy fine sand	0-0.8	0.01	0.45±0.08	3.69±0.08	2.332±0.196	2.96±5.72
	Sandy clay loam	0.8-1.5	0.043	0.38±0.07	2.81±0.43	2.210±0.172	2.44±4.19
	Sandy loam	1.5-2.4	0.02	0.43±0.08	3.44±0.51	2.469±0.330	1.66±2.84
	Loamy sand	2.4-2.5	0	0.35±0.06	3.77±0.53	1.980±0.265	2.03±3.11
	Sand	2.5-2.75	0	0.34±0.04	3.73±0.53	2.730±0.372	5.42±8.86
	Loamy sand	2.75-2.84	0	0.35±0.06	3.77±0.53	1.980±0.265	2.03±3.11
	Sand	2.84-2.9	0	0.34±0.04	3.73±0.53	2.730±0.372	5.42±8.86
WL1	Clay	0-0.3	0.065	0.56±0.09	1.37±0.19	1.293±0.092	0.17±0.26
	Sandy clay	0.3-0.9	0.06	0.44±0.07	2.85±0.36	1.416±0.125	0.21±0.38
	Clay	0.9-2.0	0.103	0.42±0.03	1.55±0.21	1.187±0.065	0.19±0.42
	Sandy clay loam	2.0-2.8	0.075	0.49±0.07	2.34±0.33	1.598±0.227	0.13±0.28
	Sandy clay	2.8-3.8	0.081	0.43±0.06	2.60±0.35	1.266±0.134	0.09±0.19



	Sandy clay loam	3.8-4.0	0.071	0.40±0.05	2.69±0.37	1.291±0.137	0.12±0.24
	Sandy clay loam	0-0.2	0.03	0.41±0.07	3.22±0.45	1.502±0.151	0.30±0.57
WL2	Sandy clay	0.2-0.6	0.01	0.37±0.06	2.56±0.39	1.422±0.081	0.09±0.19
	Sandy clay loam	0.6-3.0	0.01	0.37±0.03	1.39±0.19	1.566±0.06	0.10±0.10
	Sandy clay	0-1.4	0.09	0.49±0.09	1.27±0.15	1.470±0.111	0.22±0.14
WL3	Clay	1.4-3.6	0.105	0.53±0.05	2.03±0.29	1.285±0.100	0.17±0.36
	Loamy fine sand	3.6-3.8	0.056	0.39±0.08	2.90±0.45	1.789±0.293	1.23±2.40

646

647 **Table 4: Average root mean square error (RMSE) and related standard deviation (SD) over all scenarios for water content (Theta)**  
 648 **and chloride concentration.**

Location, Year	Theta (-)			Chloride concentration (mg l <sup>-1</sup> )		
	Average observation	Average simulation	Average RMSE	Average observation	Average simulation	Average RMSE
ST1, 2016/2019	0.25/0.22	0.23/0.23	0.06/0.04	30/6	18/22	19/19
ST2, 2016/2019	0.17/0.14	0.16/0.15	0.06/0.04	162/106	132/229	82/116
ST3, 2016/2019	0.06/0.08	0.07/0.06	0.02/0.02	42/10	6/13	58/10
WL1, 2017	0.27	0.27	0.05	31	6	59
WL2, 2017	0.13	0.15	0.02	40	3	117
WL3, 2017	0.31	0.33	0.04	12	13	9

649

650 **Table 5: Calculated average annual recharge, fraction of recharge on average annual precipitation, standard deviations of recharge**  
 651 **across the time-period 2005-2019 and 2005 – 2016 for Salamat and Waza Logone, respectively.**

Location	Average annual recharge (mm)	Fraction of average annual precipitation (%)	Standard deviation of annual recharge (mm)
ST1	7	0.9	17
ST2	9	1	29
ST3	93	12	69
WL1	28	4	32
WL2	54	8	46
WL3	6	1	48



652 **Table 6: Calculated average annual evaporation and transpiration and related standard deviations of 100 randomly accepted model**  
 653 **runs.**

Location	Average annual evaporation (mm)	Standard deviation of evaporation (mm)	Average annual transpiration (mm)	Standard deviations of transpiration (mm)	Average actual evapotranspiration (mm)
ST1	210	9	553	11	763
ST2	366	22	388	27	754
ST3	137	12	552	11	689
WL1	344	20	317	23	661
WL2	146	14	477	28	623
WL3	376	12	305	10	681

654